

Lea Kremer^{1*}, Fabian Falk¹, Litsy Hüschelrath^{1,2}, Patrick Doll^{1,2}

Investigation of the antiadhesive properties of biomimetic titanium nanostructures in fluidic flow

<https://doi.org/10.1515/cdbme-2023-1180>

Abstract: Within this work, the bacterial adhesion on biomimetic titanium nanostructures is investigated in fluidic flow. The motile, gram-negative bacteria strain *Escherichia coli* was used for the experiments and was incubated on nanostructured titanium, polished titanium and on the wings of the dragonfly *Neurobasis kaupi*. After incubation period different flow velocities have been applied and the reduction of adhered bacteria was determined via fluorescence microscopy. Results show that nanostructured titanium surfaces have the ability to reduce the bacterial contamination as it is for the dragon fly wings used in this study. This behavior can also be predicted by analyzing the bearing area of the nanotopography which describes the actual part of the topography which is in contact to the bacteria.

Keywords: nanostructured titanium, *Escherichia coli*, *Neorbasis kaupi*, bacterial adhesion, bearing area.

1 Introduction

Bacterial infections associated with medical implants are a major problem in modern implantology [1]. Bacterial adhesion to implant surfaces and the associated biofilm formation is dependent on many different factors, e.g. environmental factors such as temperature, pH, surface properties such as

topography, chemical composition amongst others [2]. When bacteria are in moving fluids, also other factors such as fluid velocity and resulting shear forces influence adhesion. Adhesion mechanisms under flow are particularly interesting when it comes to the use of implants in the oral cavity or implant used in the cardiovascular system. Especially dental implants are at constant risk of infection due to the omnipresence of germs in the oral cavity [3].

To be able to make a prediction about potential bacterial adhesion on a surface subject to a fluidic flow, the technical bearing area or bearing surface fraction (Abbott-Firestone curve) can be a useful tool. The effective (biological) bearing area is the potential contact area that results when the roughness profile is limited to a defined fraction [4]. The bearing curve can be used to analyze how much contact area a surface would have with an overlying flat surface, based on the roughness profile [5]. This basic mechanics can also be seen when it comes to bacterial adhesion e.g. on artificial silicon nanostructures where nanotopography directly influences the bacterial adhesion forces due to the availability of contact area [6].

To demonstrate this mechanics on real world implant surfaces, we performed this study comparing polished titanium surfaces with biomimetic titanium nanostructures and the antiadhesive example known from nature, nanostructures from dragon fly wings [7].

2 Materials & Methods

2.1 Sample Preparation

Titanium grade 23 samples were cut from a bar (diameter of 8 mm) into individual disks with a thickness of 2 mm each by wire cutting. Samples were ground with silicon carbide grinding paper and mechanically/chemically polished to a mirror like finish. One set of samples was set aside as a control group (Polished). The other samples were oxidized in a special

*Corresponding author: **Patrick Doll:** Karlsruhe Institute of Technology, Institute of Microstructure Technology, Hermann-von-Helmholtz-Platz 1, 76344 Eggenstein-Leopoldshafen, Germany and nanoshape GmbH, Haid-und-Neu-Str. 7, 76131 Karlsruhe, email: patrick.doll@nanoshape.de Germany

Lea Kremer, Fabian Falk: Karlsruhe Institute of Technology, Institute of Microstructure Technology, Hermann-von-Helmholtz-Platz 1, 76344 Eggenstein-Leopoldshafen, Germany

Litsy Hüschelrath: Karlsruhe Institute of Technology, Institute of Microstructure Technology, Hermann-von-Helmholtz-Platz 1, 76344 Eggenstein-Leopoldshafen, Germany and nanoshape GmbH, Haid-und-Neu-Str. 7, 76131 Karlsruhe, Germany

polytetrafluoroethylene-lined high-pressure autoclave for 24 h (Oxidized).

In addition, the wings of the dragonfly *Neurobasis kaupi* were cut in approx. 8 mm x 8 mm pieces (Dragonfly) and attached to a blank sample for handling. For Scanning Electron Microscopy and Atomic Force Microscopy only the wing pieces were sputter coated with silver before the measurements (k575x, Emtech, Germany).

2.2 Sample Characterization

2.2.1 Scanning Electron Microscopy

Scanning Electron Microscopy (SEM) analysis was performed using an Extra High Tension (EHT) between 1.5 and 10 kV at working distances in the range of approx. 2 to 8 mm (Supra VP 60, Zeiss, Germany).

2.2.2 Atomic Force Microscopy

In "Tapping Mode in Air" with a high frequency cantilever (frequency = 150 kHz and force = 7.4 Nm), the titanium specimens and dragonfly wings are examined for their roughness parameters and bearing area using Atomic Force Microscopy (AFM, Bruker Veeco Dimension Icon). The scan range was set to 10 x 10 μm^2 , 3 x 3 μm^2 and 1 x 1 μm^2 with 512 Samples per Line.

2.3 Biological Preparation

Bacterial tests were performed using *Escherichia coli* (DSM498), a typical model strain representing gram-negative rod-shaped, motile bacteria. Different samples were incubated in the working bacteria culture (optical density OD500 = 0.05) for 1 h at 37 °C in Luria-Bertani Miller medium. After incubation samples were gently dipped in Phosphate Buffered Saline (PBS) and stained with a 10 $\mu\text{g}/\text{ml}$ DAPI solution for 30 min before the fluidic experiments.

2.4 Flow chamber

The flow chamber (Fig. 1) consists of a main section measuring 100 mm x 50 mm x 10 mm made of polytetrafluoroethylene, a cover plate that secures a glass slide, and a ring seal. The cover plate, slide, and gasket are connected to the main body by M4 stainless steel screws.

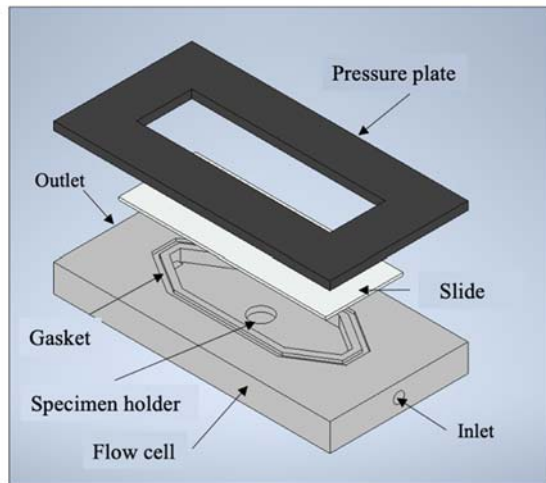


Figure 1: Schematic CAD drawing of the flow chamber design.

In the main part, there is a 70 mm long, 19 mm wide and 4 mm deep recess with a countersunk hole ($d = 8 \text{ mm}$) in the centre for the specimen.

At each of the long ends there is an opening as inlet and outlet, respectively, which are connected by screw-in connections ($d = 2.5 \text{ mm}$) for silicone tubes ($d = 2 \text{ mm}$). An attached peristaltic pump (Reglo ICC, Ismatec, Germany) generated a laminar flow velocity between 6 $\mu\text{m}/\text{s}$ and 750 $\mu\text{m}/\text{s}$ inside the inner chamber.

One sample at a time was placed inside the chamber and the chamber was filled with PBS. The flow rate was consistently increased and images were taken in between with a microscope (Axiolab 5, Zeiss, Germany). Resulting images were then used to determine the quantity of adhered bacteria.

2.5 Calculation of the Adhesion Force

The adhesion force of a bacteria can be described as the fluidic shear force (F_i) it endures close to a wall. To calculate this shear force the interpolated equation (Eq. 1) for rod-shaped objects after Wiklund et al 2018 [8] was used.

$$F_i = f_i \left(\frac{H}{R} \right) * 6 * \pi * \eta * S * H * R \quad (1)$$

It contains the Goldman factor f_i , as already described in [8], wall distance H , object radius R , the fluids viscosity η and the shear rate S . The force must be calculated for two cases:

1. The bacteria lies vertically to the fluid flow
2. The bacteria lies parallel to the fluid flow

3 Results & Discussion

The results of surface characterization can be found in **Fig 2**. The SEM images show an even and smooth topography for the polished titanium surface. The oxidized surface shows evenly distributed nanocrystals, similar to the structures on the dragonfly wings, but smaller. The height profile (Fig. 2 b) shows that the nanocrystals on the oxidized surface are smaller in height and closer together than the structures on the dragonfly wings. These geometries are also represented within the bearing area analysis in **Fig. 3**.

The Abbott-Firestone curve for the polished titanium sample displays a steady flat line. It can be assumed that this surface offers a lot of potential adhesion surface for the bacteria. For the oxidized surfaces, the Abbott-Firestone curve shows the height distribution of the small but regular nanocrystal structures very well and it can be estimated that the adhesion surface may be decreased compared to the polished surface. The curve of the dragonfly wing surface shows some very high peaks and deep valleys. These irregular height differences create a very rough surface topography. The potential adhesion area is smaller than for the other surfaces, as it extends over a wider height difference.

The amount of adhered bacteria on the different surfaces can be found in **Fig. 4**. The blue dotted line marks the flow rate at 22 $\mu\text{m/s}$, the values of salivary flow at rest.

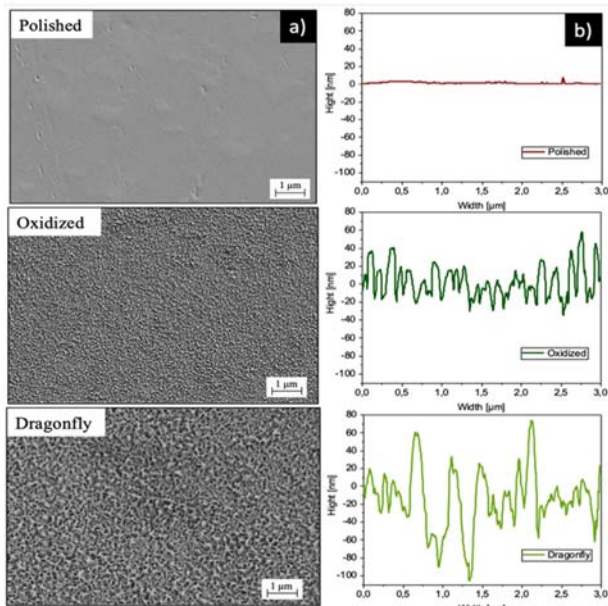


Figure 2: a) Scanning Electron Microscopy images of the polished and oxidized titanium, as well as the dragonfly wing at 10.000x magnification b) height profile of a $3 \times 3 \mu\text{m}$ area on the different surface samples

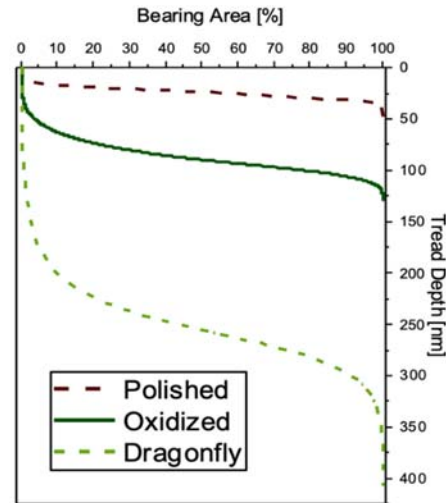


Figure 3: Bearing area of a $3 \times 3 \mu\text{m}$ area in % of the polished and oxidized titanium, as well as the dragonfly wing in an Abbott-Firestone curve.

Initially, the most bacteria grew on the polished titanium surfaces as it could be expected due to the bearing area analysis while the least amount of bacteria was found on the nanostructured titanium surface. With increasing flow rate the amount of bacteria is reduced on all surfaces respectively. The largest decrease for higher flow rates was found on the dragonfly wings.

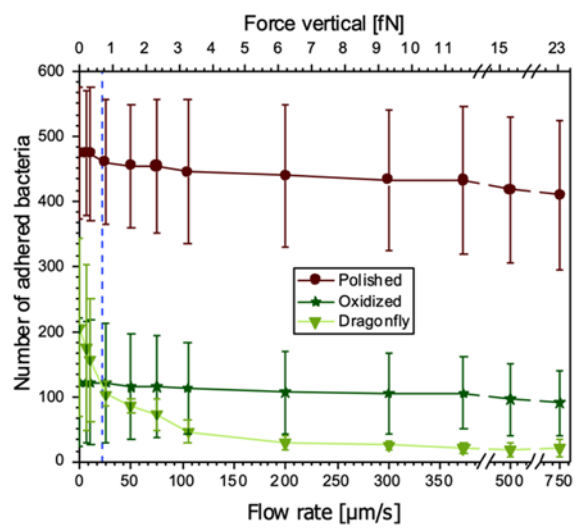


Figure 4: Reduction of adhered *E. coli* with increasing flow rate. The blue dotted line marks salivary flow at rest.

Conclusion

Nanostructured titanium surfaces fabricated by a hydrothermal oxidation method show similar antiadhesive effects like the natural nanostructures found on dragonfly wings. These results look promising for the development for novel implant surfaces. Yet, the antiadhesive properties of the nanostructured titanium have to be tested for further relevant bacterial strains and in addition, also with higher flow rates resulting in higher shear forces also influencing the bacterial adhesion.

Author Statement

Research funding: This work was funded by the German Federal Ministry of Economic Affairs and Climate Action (BMWK) and the European Social Fund (ERF) within the EXIST program (grant number: 03EFRBW233). Authors state no conflict of interest.

References

- [1] A. Tanner, M. F. J. Maiden, K. Lee, L. B. Shulman, and H. P. Weber, "Dental implant infections," *Clin. Infect. Dis.*, vol. 25, no. 2 SUPPL., pp. 213–217, 1997, doi: 10.1086/516243.
- [2] F. Song, H. Koo, and D. Ren, "Effects of material properties on bacterial adhesion and biofilm formation," *J. Dent. Res.*, vol. 94, no. 8, pp. 1027–1034, 2015, doi: 10.1177/0022034515587690.
- [3] R. J. Lamont and H. F. Jenkinson, *Oral Microbiology at a Glance*. Wiley-Blackwell, 2010.
- [4] V. S. Radchik, B. Ben-Nissan, and W. H. Müller, "Semi-Graphical Methodes for the Calculation of Real Areas of Loaded Contact by Means of Abbott-Firestone Bearing Curve," vol. 124, 2002, doi: 10.1115/1.1396345.
- [5] M. Stewart, "A NEW APPROACH TO THE USE OF BEARING AREA CURVE," 1990.
- [6] P. W. Doll *et al.*, "Influence of the Available Surface Area and Cell Elasticity on Bacterial Adhesion Forces on Highly Ordered Silicon Nanopillars," *ACS Omega*, vol. 7, no. 21, pp. 17620–17631, 2022, doi: 10.1021/acsomega.2c00356.
- [7] C. M. Bhadra *et al.*, "Antibacterial titanium nano-patterned arrays inspired by dragonfly wings," *Sci. Rep.*, vol. 5, pp. 1–12, 2015, doi: 10.1038/srep16817.
- [8] K. Wiklund, H. Zhang, T. Stångner, B. Singh, E. Bullitt, and M. Andersson, "A drag force interpolation model for capsule-shaped cells in fluid flows near a surface," *Microbiol. (United Kingdom)*, vol. 164, no. 4, pp. 483–494, Apr. 2018, doi: 10.1099/mic.0.000624.